

ENGINEERING JOURNAL

Article

Removal of Paraquat from Aqueous Solutions onto Zeolite LTL

Wilaiporn Insuwan^{1,a,*} and Kunwadee Rangriwatananon^{2,b}

¹ Faculty of Agriculture and Technology, Rajamangala University of Technology Isan Surin Campus, Surin 32000, Thailand

² School of Chemistry, Institute of Science, Suranaree University of Technology, Nakhon Ratchasima 30000, Thailand

*Email: wi_insuwan@hotmail.com

Abstract. Zeolite LTL (K_LTL and H_LTL) was used as adsorbent for the adsorption of herbicide paraquat from an aqueous solution. The characterization of zeolite LTL has been carried out through various techniques: X-ray diffraction, X-ray fluorescence spectroscopy, Fourier transform infrared spectroscopy and surface analysis. The adsorption occurred through cation exchange and the results showed that the adsorption capacity of paraquat onto K_LTL (161.71 mg/g) is higher than H_LTL (25.67 mg/g). These results can be explained by the amount of Al in the structure of zeolite and affinities of negative sites in zeolite and extra-framework cations (K^+ and H^+). The equilibrium data was best adjusted using the Langmuir model which has high correlation coefficient values (0.99).

Keywords: Paraquat, zeolite LTL, removal, Langmuir isotherm.

ENGINEERING JOURNAL Volume 21 Issue 2

Received 8 May 2016

Accepted 19 August 2016

Published 31 March 2017

Online at <http://www.engj.org/>

DOI:10.4186/ej.2017.21.2.15

1. Introduction

Paraquat (1,1'-dimethyl- 4,4' dipyridinium dichloride (Fig. 1) is the most widely used herbicide in the world. Recently, paraquat concentrations of between 1.5-18.9 $\mu\text{g/L}$ and 9.3-87.0 $\mu\text{g/L}$ were found in the ground and surface water in Thailand, respectively [1]. Although at very low concentrations, these quantities can affect humans. Mojović et al. [2] reported that the maximum permissible paraquat concentration in drinking water and surface water is 0.1 $\mu\text{g/L}$ and 1-3 $\mu\text{g/L}$, respectively. Paraquat has high solubility in water thus it can easily contaminate water. Moreover, contact with the skin or eyes has adverse effects on humans and animals. A convenient method of removal paraquat is adsorption because it is simple, efficient, and inexpensive. From a review of the literature it was found that siliceous compound [3], clay [4-5], bentonite [6], diatomaceous earth [7] and zeolite Y (NaY)[8] were reported as adsorbents for paraquat removal. Rongchapo et al. [9] reported that the exchange capacity of paraquat depends on the Si/Al ratio. They found that NaY (Si/Al ratio of 2.2) has a higher exchange capacity than NaBEA (Si/Al ratio of 14.2). Recently, Alumina-supported LTL have been fabricated using electrospinning technique used as an adsorbent for methylene blue (MB) removal where the maximum adsorption capacity is 30 mg/g [10]. This number is lower than pure zeolite LTL (72mg/g). They described that LTL zeolite embedded inside the fibers lead to limit space for dye adsorbed. Point of my view, if LTL zeolite can be removed MB that larger in size than PQ, LTL zeolite might have been also suitable for PQ removal. Zeolite LTL is hexagonal with unit cell dimensions equal to 18.4 Å and c equal to 7.5 Å, with space group P6/mmm and the chemical composition of zeolite LTL is $\text{K}_9(\text{AlO}_2)_9(\text{SiO}_2)_{27}\cdot 22\text{H}_2\text{O}$ [11]. Zeolite LTL is usually formed with the ratio Si/Al of between 3 and 6, it is can be synthesized to low-silica LTL phases with Si/Al equal to 1 [12]. Generally, zeolite frameworks are typically anionic, and charge compensating cations populate the pores to maintain electrical neutrality. These cations can participate in ion exchange with organic cations, water, and dye molecules. Several studies have been reported that zeolite LTL have been widely used in catalysis [13], sorption of dyes [14] and host materials [15]. In this study zeolites LTL (potassium form (K_LTL) and proton form (H_LTL)) were used as an alternative adsorbent for adsorption of paraquat in aqueous solution that only a few studies were reported.

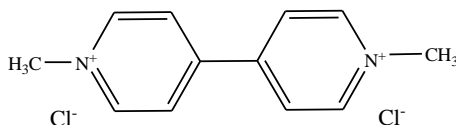


Fig. 1. Structure of Paraquat (1,1'-dimethyl- 4,4' dipyridinium dichloride).

2. Experimental Section

2.1. Materials and Chemicals

Zeolite LTL was air dried at 110 °C before use. This paper investigated the adsorption of zeolite LTL in potassium form (K_LTL) and proton form (H_LTL). Analytical grade paraquat (1,1'-dimethyl- 4,4' dipyridinium dichloride, PQ) was purchased from Sigma-Aldrich and used as an adsorbate. Zeolite LTL (K_LTL and H_LTL) crystals were synthesized by a method modified from [14]. The aluminum hydroxide was dissolved in boiling potassium hydroxide until the solution became clear and was later added to the mixture of Ludox HS 40 colloidal silica and water. The resulting mixture was stirred for few minutes to obtain a homogeneous mixture gel. The starting gel was then transferred into a Teflon-lined autoclave for crystallization at 180 °C for 2 days without stirring. After crystallization, the Teflon-lined autoclave was cooled in cold water before opening. The product was washed with DI-water until the pH of liquid was close to 7-8. Finally, the crystalline solid was dried for overnight at 100 °C in an air oven. H_LTL was prepared by transforming K_LTL to NH₄LTL by ion-exchanging K_LTL with 1 M NH₄NO₃ solution and subsequently calcining NH₄LTL at 723 K for 4 h to decompose NH₄⁺ ions to H⁺ and NH₃.

2.2. Characterization

The synthesized zeolites were analyzed through various techniques: X-ray powder diffraction (XRD) was used with Model D5005, Bruker, CuK α radiations scanning from 3-50° at a rate of 0.05 °/s with current 35 mV and 35 mA. The experimental XRD patterns obtained from the products were compared with those reported in a collection of simulated XRD patterns [16]. The chemical compositions were analyzed by energy dispersive XRF (EDS Oxford Instrument ED 2000) with Rh X-ray tube as a target with a vacuum medium. The framework was also confirmed by FT-IR (Spectrum GX, Perkin-Elmer) with the KBr pellet technique in the range between 4000 and 400 cm⁻¹. Particle size distribution was determined by Laser Diffraction Particle Size Analyzer (DPSA) (Malvern Instruments, Mastersizer 2000) with the sample dispersed in distilled water and analyzed by a He-Ne laser. The specific surface area and micropore surface area were evaluated by nitrogen gas adsorption at 77 K using automated volumetric equipment (Autosorb 1-Quantachrome Instrument), USA. The determination of surface areas was calculated by the BET (Brunauer–Emmett–Teller) method. The t-plot method was carried out to measure the micropore surface area.

2.3. Adsorption Isotherm Studies

Aqueous solutions of paraquat (PQ) were prepared by dissolving PQ in distilled water with a concentration of 50-500 ppm and initial pH of 11.0. The adsorption of the PQ was performed by shaking 0.05 g of the zeolite LTL in 25 mL of the PQ aqueous solutions with varying concentrations at 30 °C for 24 h. A preliminary of the adsorption study showed that adsorption of the dyes was almost complete within 6–8 h. A 24 h period was then chosen for conducting the adsorption tests to ensure that equilibrium was attained. After the equilibration, the solid phases were separated from the liquid phases by centrifugation. The concentration of the PQ was determined spectrophotometrically by measuring absorbance at 237 nm for maximum absorption of PQ. The data obtained from the adsorption tests were used to calculate the adsorption capacity, q_e (mg/g), of the adsorbent by a mass balance relationship.

$$q_e = \frac{(C_0 - C_e)V}{m} \quad (1)$$

where q_e (mg/g) is the amount of PQ adsorbed at equilibrium. v (L) is the volume of the liquid phase, and m (g) is the mass of the solid phase. C_0 (mg/L) and C_e (mg/L) are concentrations of PQ in solution at the initial stage and concentration of PQ in the liquid phase at equilibrium, respectively. Isotherm data were analyzed using Langmuir and Freundlich adsorption equations. The Langmuir equation is as follows [14]:

$$q_e = \frac{q_m K_L C_e}{1 + K_L C_e} \quad (2)$$

where K_L (g/mg) is the Langmuir constant of adsorption. The linear form of the Langmuir model is expressed as the following Eq. (3):

$$\frac{C_e}{q_e} = \frac{1}{q_m} C_e + \frac{1}{K_L q_m} \quad (3)$$

The Freundlich isotherm is introduced as an empirical model, where q_e represents the amount adsorbed per amount of adsorbent at the equilibrium (mg/g), C_e represents the equilibrium concentration (mg/L), K_F and n are Freundlich constants which correspond to adsorption capacity and adsorption intensity, respectively [7].

$$q_e = K_F C_e^{\frac{1}{n}} \quad (4)$$

The linear form of the Freundlich model is expressed in the following Eq. (5):

$$\log(q_e) = \log K_F + \frac{1}{n} \log C_e \quad (5)$$

3. Results and Discussion

3.1. X-ray Diffraction (XRD)

To characterize K_LTL and H_LTL, the XRD patterns were compared with those reported in the collection of simulated XRD patterns [16]. The XRD patterns of both forms of zeolite LTL show the characteristic reflection bands at 2θ are equal to 5.5, 19.4, 22.7, 28.0, 29.1 and 30.7, respectively. Figure 2 shown the intensity of H_LTL is lower than that of K_LTL. A possible explanation of this observation is that the heat treated sample in the calcination step led to the destruction of the crystalline framework.

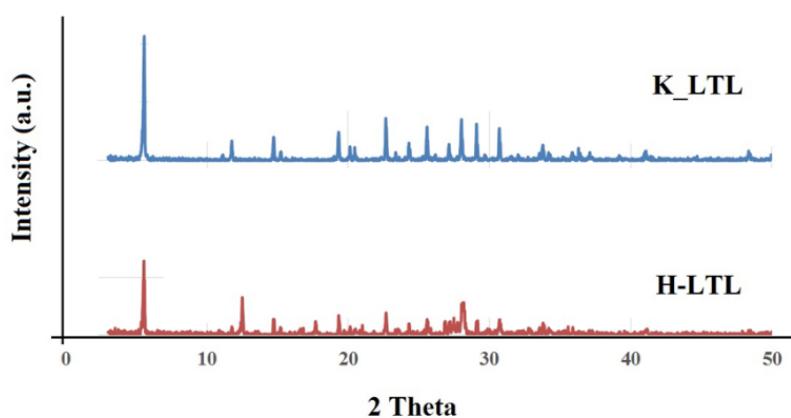


Fig. 2. XRD patterns of K_LTL and H_LTL.

3.2. FTIR Determination

The FTIR spectra of PQ adsorb K_LTL and H_LTL crystals as shown in Fig. 3. Generally, the triplet band in the range 1099 - 1026 cm^{-1} correspond to the report of [15] indicating that the internal vibrations of T-O-T (T = Si, Al) are tetrahedral. Sharp bands around 725 and 770 cm^{-1} were the main characteristics of external or internal symmetric stretching and the band around 608 cm^{-1} showed the band characteristics of double-six-ring vibration. The bands at 482 cm^{-1} were assigned to the T-O bending mode [17]. The comparison of PQ adsorption on K_LTL and H_LTL and the enlargement of the 1200-1800 cm^{-1} region illustrate that many bands belonging to the intercalated PQ are well-resolved. However, in the case of PQ, adsorption of H_LTL in the 1200-1800 cm^{-1} region could not be detected. These results demonstrate that the affinity of PQ for adsorption to the H_LTL is weaker than that observed for K_LTL. Another explanation may be that PQ cannot adsorb H_LTL zeolite. A characteristic set of bands between 1200-1800 cm^{-1} may be assigned to the C-C stretching mode and the C-H deformation mode in the pyridine ring as reported by [8]. The 1645 cm^{-1} band can be assigned to the stretching mode of the pyridine ring [19]. In addition, the stretching mode of C=N band of PQ adsorption on K_LTL appeared at 1571 cm^{-1} . However, it can be seen that the intercalation of PQ causes three of its bands to shift, band 1506 cm^{-1} , 1444 cm^{-1} , and 1336 cm^{-1} . Similar reports in the literature have shown that PQ-host (zeolite LTL) interactions influence the conformation of the pyridine ring which causes a shift in the spectra [19].

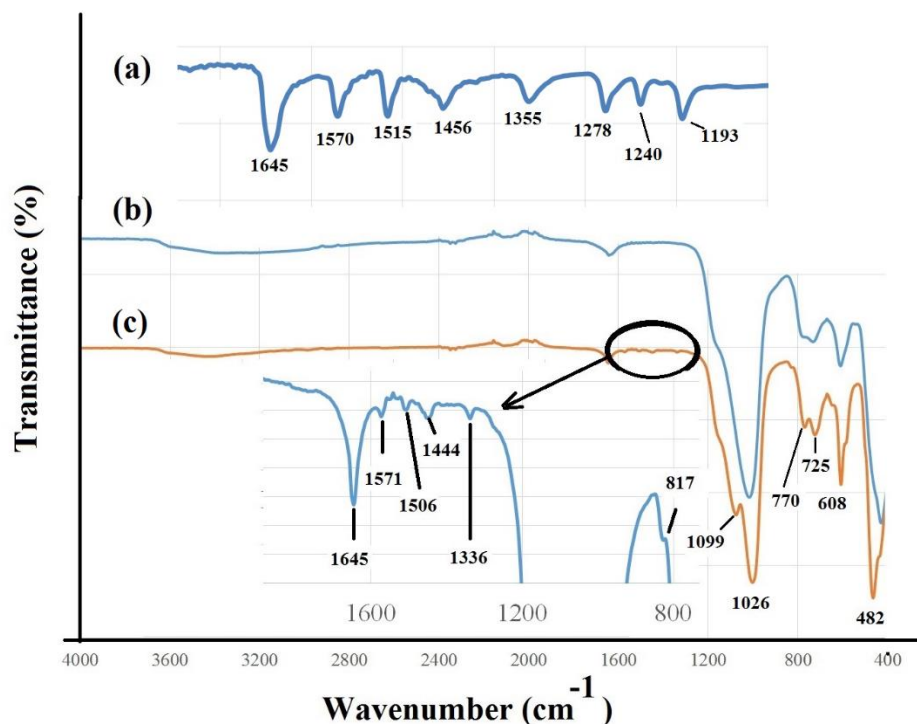


Fig. 3. (a) FTIR spectra of paraquat dichloride with an enlargement region of 1000-2000 cm^{-1} ; (b) paraquat adsorp on H_LTL; and (c) paraquat adsorp on K_LTL.

3.3. Textural Properties of Zeolite LTL

Information of the textural properties of zeolite LTL are summarized in Table 1. The surface area and micropore surface area of H_LTL zeolite were increased when compared with K_LTL zeolite. This result can be explained by the smaller size of the extra-framework cation of H^+ ion compared to K^+ ion, resulting in the enlargement of space for N_2 adsorption [14]. Moreover, the higher the Si/Al ratio for H_LTL, the smaller the amount of Al concentrations in the zeolite structure and consequently the smaller the amount of exchangeable cation present in the adsorbent. Brian Hennessy and co-worker [19] reported that Methyl Viologen (Paraquat dichloride) could be inserted into the self-synthesized potassium zeolite LTL more easily than into the commercial zeolite LTL. They described the higher surface area and the greater of micropore as providing more free space for Methyl Viologen occupy. However, in this work we focus on the extra-framework cation (K^+ and H^+ ion). Figure 4 shows the adsorption isotherm of PQ on zeolite LTL and the monolayer adsorption capacity was calculated from the langmuir equation (Fig. 5) that shows 166.71 mg/g and 25.67 mg/g in K_LTL and H_LTL, respectively (Table 2). In addition, adsorption data for the PQ on LTL was fitted to the linear form of Freundlich isotherm (Eq. (5)). The values of K_F was related to the degree of adsorption that the PQ adsorbed on K_LTL having the greater than PQ adsorbed on H_LTL. This mean that it has higher affinity between PQ and K_LTL as compared to the H_LTL. The trend for adsorption capacity is similar to the trend for Al content (Table 1), suggesting that the main factor in the adsorption depends on the Si/Al ratio. The higher the amount of Al concentrations, the higher the amount of K^+ ions present in the adsorbent. Because the Si/Al ratio of K_LTL is lower than that of H_LTL, K_LTL has a higher exchange capacity. Because of the transformation of K_LTL to NH_4LTL process, NH_4LTL was calcined in high temperature, resulting in deammoniation and generation of Bronsted acidic bridging protons in the framework. In the meantime, aluminium is removed from the framework, silicon atoms can be migrated to fill these empty sites [20]. Furthermore, they have different ionic sizes and different affinities for the negative charge sites in zeolite. The potassium ion is bound in zeolite through the electrostatic attraction force while the hydrogen ion is usually bound though hydrogen bonding [21]. The hydrogen bonding becomes very strong as it binds to the negative charge site in the zeolite. Thus zeolite H_LTL hardly exchanges with PQ more than that K_LTL.

Table 1. Textural properties of zeolite LTL.

Zeolite LTL	Surface area (m ² /g)	Micropore surface area (m ² /g)	Particle size (μm)	Si/Al ratio
K_LTL	320	298	2.17	3.14
H_LTL	404	369	5.10	5.10

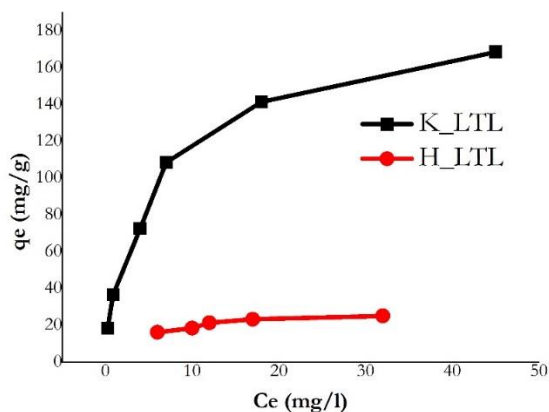


Fig. 4. Adsorption isotherms of paraquat onto zeolite K_LTL and H_LTL.

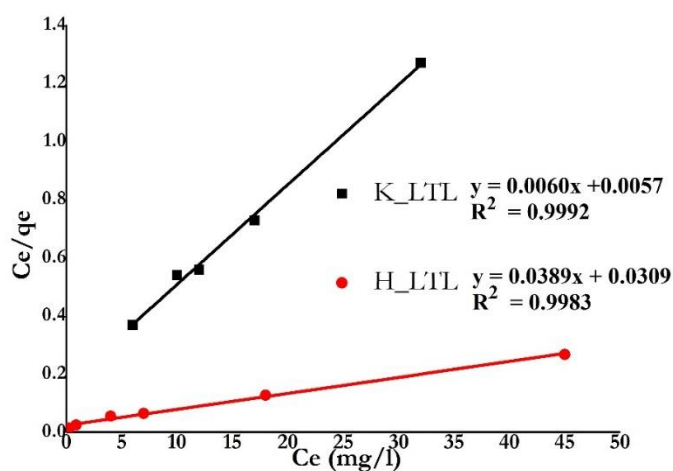


Fig. 5. Linear plot of Langmuir isotherm of paraquat onto zeolite K_LTL and H_LTL.

Table 2. Models isotherm constants for the paraquat adsorption onto zeolite LTL.

Zeolite LTL	Langmuir adsorption isotherm			Freundlich adsorption isotherm		
	q _m (mg/g)	K _L (L/mg)	R ²	K _F (mg ^{1-1/n} /L ^{1/ng})	n	R ²
K_LTL	166.71	1.05	0.9992	2.76	0.63	0.9759
H_LTL	25.67	1.26	0.9983	1.86	0.98	0.9157

Comparisons of adsorbent types and maximum capacity are shown in Table 3. As found in the review of the literature and as our results also reveal K_LTL could be applied as adsorbent for the removal PQ as well.

Table 3. Comparisons of maximum adsorption capacity on various adsorbents which obeyed the Langmuir equation.

Adsorbent	Maximum adsorption capacity (mg/g)	References
Heat treated bentonite, calcined at 400 °C	100	[5]
Heat treated bentonite, calcined at 600 °C	28	[5]
Treated diatomaceous	17.06	[6]
RHS	18.9	[8]
MCM-41	21.3	[8]
NaY	185.2	[8]
NaBEA	122.0	[8]
Kaolin	5.447	[22]
Phillipsite–faujasite tuff in Na form	4.67-7.02	[23]
K_LTL	166.71	this work
H_LTL	25.67	this work

We Consider that the change in Gibbs free energy (ΔG°) of the adsorption process is related to the equilibrium constant by the following Eq. (6) (Insuwan and Rangsiwatananon 2014) [14].

$$\Delta G^\circ = -RT \ln K_L \quad (6)$$

where R is the gas constant (8.314 J/mol K), T is temperature (K), and K_L is the adsorption constant in the Langmuir isotherm. From the data, the change in Gibbs free energy (ΔG°) of adsorption of PQ on K_LTL and H_LTL is -0.13 and -0.58 kJ/mol, respectively. The negative values of ΔG° imply that the reaction occurs in the direction where adsorption takes place and shows the spontaneous nature of the adsorption processes.

4. Conclusion

The present study was conducted to evaluate the possibility of using K-form and H-form of zeolite LTL for PQ removal from aqueous solutions. The results show that zeolite K_LTL has a larger adsorption capacity than H_LTL, owing to amount of Al in the structure of zeolite. In addition, the affinities of negative sites in zeolite and the extra-framework cation (K^+ and H^+) should be considered. The analysis of the FTIR spectrum of the PQ-adsorbent confirmed that the sorption is controlled by a cation exchange. Furthermore, the Langmuir model appears to fit the data better than the Freundlich model for describing the adsorption behavior of PQ onto zeolite LTL. The above results suggest that the zeolite in potassium form (K_LTL) could be used as an effective adsorbent for the removal of PQ from ground, surface water and soil water.

Acknowledgments

The researchers would like to acknowledge Rajamangala University of Technology Isan Surin Campus and Suranaree University of Technology for their financial support to enable this research work to be completed successfully.

References

- [1] M. S. F. Santos, G. Schaule, A. Alves, and L. M. Madeir, "Adsorption of paraquat herbicide on deposits from drinking water networks," *Chemical Engineering Journal*, vol. 229, pp. 324-333, 2013.
- [2] Z. Mojović, P. Banković, A. Milutinović-Nikolić, J. Dostanić, N. Jović-Jovčić, and D. Jovanović, "Al, Cu pillared clays as catalysts in environmental protection," *Chemical Engineering Journal*, vol. 154, pp. 149-155, 2009.
- [3] M. Brigante and P. C. Schulz, "Adsorption of paraquat on mesoporous silica modification with titania: effects of pH, ionic strength and temperature," *Journal of Colloid and Interface Science*, vol. 363, pp. 355-361, 2011.
- [4] D. C. Ricketts, "The microbial biodegradation of paraquat in soil," *Pesticide Science*, vol. 55, no. 5, pp. 596-614, 1999.
- [5] Y. Seki and K. Yurdakoç, "Paraquat adsorption onto clays and organoclays from aqueous solution," *Journal of Colloid and Interface Science*, vol. 287, pp. 1-5, 2005.
- [6] D. Ait Sidhoun, M. M. Socías-Viciano, M. D. Ureña-Amate, A. Derdour, E. González-Pradas, and N. Debbagh-Boutarbouch, "Removal of paraquat from water by an Algerian bentonite," *Applied Clay Science*, vol. 83-84, pp. 441-448, 2013.
- [7] W. T. Tsai, K. J. Hsien, Y. M. Chang, and C. C. Lo, "Removal of herbicide paraquat from an aqueous solution by adsorption onto spent and treated diatomaceous earth," *Bioresource Technology*, vol. 96, pp. 657-663, 2005.
- [8] H. Nur, A. F. N. A. Manan, L. Wei, M. N. M. Muhid, and H. Hamdan, "Simultaneous adsorption of a mixture of paraquat and dye by NaY zeolite covered with alkylsilane," *Journal of Hazardous Materials*, vol. 117, pp. 35-40, 2005.
- [9] W. Rongchapo, O. Sophiphun, K. Rintramee, S. Prayoonpokarach, and J. Wittayakun, "Paraquat adsorption on porous materials synthesized from rice husk silica," *Water Science and Technology*, vol. 68, pp. 863-869, 2013.
- [10] G. P. Singaravel and R. Hashaikeh, "Fabrication of electrospun LTL zeolite fibers and their application for dye removal," *Journal of Materials Science*, vol. 51, pp. 1133-1141, 2016.
- [11] D. W. Breck, *Zeolite Molecular Sieves: Structure, Chemistry and Use*. New York: Wiley, 1974, pp. 113-156.
- [12] C. S. Carr and D. F. Shantz, "Synthesis of high aspect ratio low-silica zeolite L rods in oil/water/surfactant mixtures," *Chemistry of Materials*, vol. 17, pp. 6192-6197, 2005.
- [13] S. Trakarnroek, S. Jongpatiwut, T. Rirksomboon, S. Osuwan, and D.E. Resasco, "n-octane aromatization over Pt/KL of varying morphology and channel lengths," *Applied Catalysis A: General*, vol. 313, pp. 189-199, 2006.
- [14] W. Insuwan and K. Rangriwatananon, "Evaluation of adsorption of cationic dyes on H-LTL and K-LTL zeolite," *Journal of Porous Materials*, vol. 21, no. 3, pp. 345-354, 2014.
- [15] V. Vohra, A. Devaux, L.-Q. Dieu, G. Scavia, M. Catellani, G. Calzaferrri, and C. Botta, "Energy transfer in fluorescent nanofibers embedding dye loaded zeolites L crystals," *Advanced Materials*, vol. 21, pp. 1146-1150, 2009.
- [16] M. M. J. Treacy, J. B. Higgins, and R. Von Ballmons, *Collection of Simulated XRD Power Diffraction Pattern of Zeolites*. Elsevier, 2001, pp.218-221.
- [17] W. Insuwan and K. Rangriwatananon, "Morphology-controlled synthesis of zeolite L and physicochemical properties," *Engineering journal*, vol. 16, no. 3, pp. 1-12, 2012.
- [18] R. Haque and S. Lilley, "Infrared spectroscopic studies of charge transfer complexes of diquat and paraquat," *Journal of Agricultural and Food Chemistry*, vol. 20, pp. 57-58, 1972.

- [19] B. Hennessy, S. Megelski, C. Marcolli, V. Shklover, C. Bärlocher, and G. Calzaferri, "Characterization of methyl viologen in the channels of zeolite L," *Journal of Physical Chemistry B*, vol. 103 (17), pp. 3340-3351, 1999.
- [20] M. Czjzek, H. Jovic, A. N. Fitch, and T. Vogt, "Direct determination of proton positions in D-Y and H-Y zeolite samples by neutron powder diffraction," *Journal of Physical Chemistry*, vol. 96, no. 4, pp. 1535-1540, 1992.
- [21] J. L. White, L. W. Beck, and J. F. Haw, "Characterization of hydrogen bonding in zeolites by proton solid-state NMR spectroscopy," *Journal of the American Chemical Society*, vol. 114, no. 15, pp. 6182-6189, 1992.
- [22] D. A. Martins, M. Simões, and L. Melo, "Adsorption of paraquat dichloride to kaolin particles and to mixtures of kaolin and hematite particles in aqueous suspension," *Journal of Water Security*, vol. 1, pp. 25-36, 2015.
- [23] K. M. Ibrahim and H. A. Jbara, "Removal of paraquat from synthetic wastewater using phillipsite-faujasite tuff from Jordan," *Journal of Hazardous Materials*, vol. 163, pp. 82-86, 2009.